1,2,4-Triphospholyl Nickel Complexes: Evidence for a Dimerization Equilibrium That Includes a $\sigma-\pi$ Rearrangement of the Triphospholyl Ligand†

Frank W. Heinemann,‡ Hans Pritzkow,§ Matthias Zeller,‡ and Ulrich Zenneck*,‡

Institut für Anorganische Chemie, Universität Erlangen-Nürnberg, Egerlandstrasse 1, 91058 Erlangen, Germany, and Institut für Anorganische Chemie, Universität Heidelberg, Im Neuenheimer Feld 270, 69120 Heidelberg, Germany

Received April 18, 2000

1-Trimethylstannyl-3,5-di(*tert*-butyl)-1,2,4-triphosphole (**2**) reacts efficiently with [$(PPh_3)_2$-$NiCl_2$] or [$(NO)(PPh_3)_2NiCl$] by elimination of Me_3SnCl and formation of 3,5-di(*tert*-butyl)-1,2,4-triphospholyl (**1**) nickel complexes. [(η^5-*t*-$Bu_2C_2P_3$)(PPh_3)NiCl] (**5**) is a half-sandwich complex that is closely related to its carbacyclic counterpart [η^5-Cp(PPh_3)NiCl]. The properties of the reaction product of [$(NO)(PPh_3)_2NiCl$] and **2**, however, differ significantly from those expected for the proposed target product [(η^5-*t*-$Bu_2C_2P_3$)(NO)Ni] (**7**). In the solid state and at low temperatures in solution, the dimeric σ-complex [μ,η^1:η^1(*t*-$Bu_2C_2P_3$)(NO)(PPh_3)Ni]$_2$ (**6**) is the only observable species and contains two additional PPh_3 ligands. On warming the solutions, dimer **6** dissociates PPh_3 reversibly to form a mixture of free PPh_3 and the piano-stool compound [(η^5-*t*-$Bu_2C_2P_3$)(NO)Ni] (**7**) as the ambient-temperature species. This temperature-dependent and fully reversible $\sigma-\pi$ rearrangement of the triphospholyl ligand **1** is unique for unsaturated P-heterocycles. The low-temperature complex **6** also exhibits an unusual coordination mode, as its topology is much more closely related to the N-heterocyclic Cp analogues pyrazolate and triazolate than to other P-heterocycles.

Introduction

Phosphorus atoms as parts of unsaturated heterocycles may replace CR fragments as isovalent and isolobal building blocks, which results in the formation of numerous organophosphorus and organometallic phosphorus compounds in which the phosphorus atom might be viewed as a *carbon copy*.[1] However, in some cases the ligating properties of oligophospha cyclopentadienyl derivatives differ significantly from those of their carbacyclic cyclopentadienyl (Cp) analogues, clear evidence of the fact that an analogy approach in the field of organophosphorus transition metal chemistry cannot explain the experimental findings completely.[2]

One fundamental difference between a phosphorus atom and a CR unit in analogous bonding situations is the lone pair of the phosphorus atom, which is absent for the carbon atom in most cases. Especially in the case of π-ligands, this may cause dramatic changes of the ligating properties, as this lone pair may come into play in ground-state structures as well as in transition states. Examples have been shown for the phospholyl ligand, which is the simplest example of a phosphorus heterocyclic analogue of the Cp ligand. Thus, phospholyl derivatives bind metals either by the phosphorus lone pair as a σ-ligand or in an η^5-fashion via the delocalized aromatic π-system, depending on the metal atom and the coligands.[3] For diphospholyl complexes an intermediate η^3-coordination mode has also been observed.[4] In recent years, a series of complexes containing the 3,5-di(*tert*-butyl)-1,2,4-triphospholyl ligand (**1**) has been synthesized. Most examples contain a terminal η^5-bonded ligand,[2,5] and a few examples are known for bridging μ,η^5-ligands,[6] including two extremely slipped triple-deckers in which **1** functions as a μ,η^5:η^2-bridge.[7] η^1-Complexes of **1** have also been reported,[8,9,10] and both coordination modes are united in binuclear μ,η^5:η^1-

† Dedicated to Professor Dieter Sellmann on the occasion of his 60th birthday.

* Corresponding author. Fax: + 49-9131-852-7367. E-mail: zenneck@chemie.uni-erlangen.de.

‡ Universität Erlangen-Nürnberg.

§ Universität Heidelberg.

(1) Dillon, K. B.; Mathey, F.; Nixon, J. F. *Phosphorus, The Carbon Copy*; John Wiley & Sons: Chichester, 1998.

(2) Clark, T.; Elvers, A.; Heinemann, F. W.; Hennemann, M.; Zeller, M.; Zenneck, U. *Angew. Chem.* **2000**, *112*, 2174−2178; *Angew. Chem., Int. Ed.* **2000**, *39*, 2087−2091.

(3) Mathey, F.; Fischer, J.; Nelson, J. H. *Struct. Bonding* **1983**, *55*, 153−201. Mathey, F. *J. Organomet. Chem.* **1994**, *475*, 25−30. Garnowskii, A. D.; Sadimenko, A. P. *Adv. Heterocyclic Chem.* **1999**, *72*, 1−77. Arliguie, T.; Ephritikhine, M.; Lance, M.; Nierlich, M. *J. Organomet. Chem.* **1996**, *524*, 293−297.

(4) Bartsch, R.; Hitchcock, P. B.; Nixon, J. F. *J. Organomet. Chem.* **1989**, *373*, C17−C20. Bartsch, R.; Hitchcock, P. B.; Nixon, J. F. *J. Chem. Soc., Chem. Commun.* **1990**, 472−474.

(5) Driess, M.; Hu, D.; Pritzkow, H.; Schäufele, H.; Zenneck, U.; Regitz, M.; Rösch, W. *J. Organomet. Chem.* **1987**, *334*, C35−C38. Bartsch, R.; Hitchcock, P. B.; Nixon, J. F. *J. Organomet. Chem.* **1988**, *356*, C1−C4. Callaghan, Ch.; Clentsmith, G. K. B.; Cloke, F. G. N.; Hitchcock, P. B.; Nixon, J. F.; Vickers, D. M. *Organometallics* **1999**, *18*, 793−795. Bartsch, R.; Hitchcock, P. B.; Nixon, J. F. *J. Chem. Soc., Chem. Commun.* **1987**, 1146. Bartsch, R.; Hitchcock, P. B.; Madden, T. J.; Meidine, M. F.; Nixon, J. F.; Wang, H. *J. Chem. Soc., Chem. Commun.* **1988**, 1475−1476.

(6) Böhm, D.; Heinemann, F.; Hu, D.; Kummer, S.; Zenneck, U. *Collect. Czech. Chem. Commun.* **1997**, *62*, 309−317. Hitchcock, P. B.; Johnson, J. A.; Nixon, J. F. *Organometallics* **1995**, *14*, 4382−4389.

(7) Elvers, A.; Heinemann, F. W.; Wrackmeyer, B.; Zenneck, U. *Chem. Eur. J.* **1999**, *5*, 3143−3153. Callaghan, C.; Nixon, J. F. Unpublished results reported by Nixon, J. F., in ref 1, p 328.

(8) Bartsch, R.; Carmichael, D.; Hitchcock, P. B.; Meidine, M. F.; Nixon, J. F.; Sillet, G. J. D. *J. Chem. Soc., Chem. Commun.* **1988**, 1615−1617.

10.1021/om000326g CCC: $19.00
Publication on Web 09/08/2000

Scheme 1

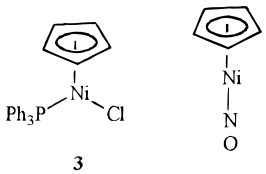

3 4

Scheme 2

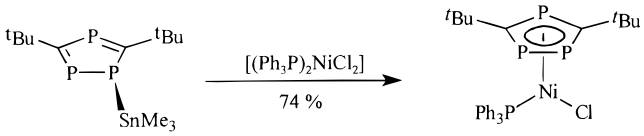

2 5

complexes.[11] As we have developed an easy access to 1-triorganylstannyl triphosphole derivatives such as 1-trimethylstannyl-3,5-di(*tert*-butyl)-1,2,4-triphosphole (**2**),[7] which is an excellent starting material for the high-yield transfer of **1**, we have started a systematic investigation to study the ligand properties of this phosphorus-rich cyclopentadienyl derivative in detail. In the case of [bis{3,5-di(*tert*-butyl)-1,2,4-triphospholyl}-Mn] for example,[2] we have shown the electronic ground state to be different from all known manganocene derivatives. Evidently, in this case the triphospholyl ligand **1** is no longer a strict analogue of Cp. In this paper we report the preparation and properties of 3,5-di(*tert*-butyl)-1,2,4-triphospholyl nickel complexes.

Results and Discussion

Our experiments initially followed the chemistry of Cp as a ligand of nickel. Targets were thus the triphospholyl analogues of the half-sandwich complexes [η^5-Cp(PPh_3)NiCl] (**3**) and [η^5- Cp(NO)Ni] (**4**), which are both stable 18-valence-electron (VE) compounds (Scheme 1).[12,13] In agreement with this expectation, the reaction of [$(PPh_3)_2NiCl_2$] with 1-trimethylstannyl-3,5-di(*tert*-butyl)-1,2,4-triphosphole (**2**) leads to the formation of [(η^5-*t*-$Bu_2C_2P_3$)(PPh_3)NiCl] (**5**) in good yield. As expected, **5** is just the triphospholyl analogue of **3** (Scheme 2). A single-crystal X-ray diffraction study established the molecular structure with an η^5-bonded triphospholyl ligand (Figure 1, Table 1). The structural findings are in good agreement with the spectroscopic properties of **5**. Spectra and structural features are in line with **3**[12] and other diamagnetic 18-VE sandwich and half-sandwich complexes of **1**.[2,5,14] However, in contrast with this nickel(II) species, the heavier elements of the nickel triad form square-planar 16-VE complexes of Pd(II) and Pt(II) with **1** as a σ-ligand.[8,9] This suggests that the differences in energy for the two principal coordination modes of **1** versus the dications of late transition metals are not very significant.

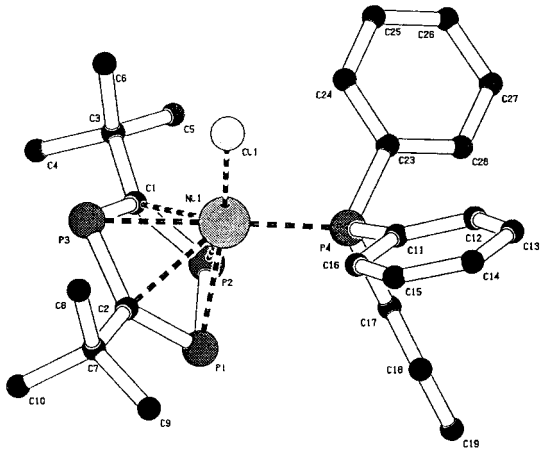

Figure 1. Molecular structure of **5** in the solid state; hydrogen atoms are omitted for clarity.

Treatment of [$(NO)(PPh_3)_2NiCl$] with 1 equiv of **2** results in the formation of a black crystalline solid **6**, whose spectroscopic properties are in agreement with the target piano-stool complex [(η^5-*t*-$Bu_2C_2P_3$)(NO)Ni] (**7**), the analogue of **4**. However, all solutions prepared from compound **6** contain 1 equiv of free PPh_3 per nickel atom. This PPh_3 cannot be removed or even reduced by recrystallization. The empirical composition of **6** is therefore [(*t*-$Bu_2C_2P_3$)(NO)(PPh_3)Ni]. Room-temperature ^{31}P and ^{13}C NMR spectra of **6** strongly favor the proposed η^5-coordination mode of ligand **1**. Furthermore, the ν(NO) frequency of 1824 cm^{-1} observed in solution reproduces nearly perfectly the value found for [(η^5-Cp)-(NO)Ni],[13] which speaks well for a linear, positively charged NO ligand that donates three electrons to the metal atom here as well. If PPh_3 is a ligand of complex **6**, this would require the NO to be a one-electron ligand to limit the electron count of the central metal to 18 VE. In contrast, the ν(NO) frequency observed for the solid is only 1751 cm^{-1}, indicating again different bonding types in the solid state and solution.

An X-ray diffraction study solved the puzzle. **6** forms a dimeric σ-complex, which indeed includes the observed PPh_3 ligand in the solid state. The correct formula of solid **6** is {μ[1:2-η-*t*-$Bu_2C_2P_3$](NO)(PPh_3)Ni}$_2$ (Figure 2, Table 2, Scheme 3).

The two equivalent nickel atoms are coordinated in tetrahedral spheres each generated by lone pairs of one of the two adjacent phosphorus atoms of the ligands **1**, one PPh_3, and one NO ligand. There is no evidence of any bonding interaction between the two metal atoms (Ni−Ni = 4.745(1) Å). The μ,η^1:η^1-bridging mode of the ligands **1** within dimer **6** is almost symmetric, and a crystallographic inversion center is located halfway between the two metal atoms. To the best of our knowledge, only one report on a related μ,η^1:η^1-bridging mode of ligand **1** has appeared in the literature, but only for a single bridging ligand and a low-yield side product, not a main product as here.[15] **6** is therefore a rare case. In contrast with most oligophospha cyclopentadienyl derivatives, triphospholyl ligand **1** seems to be much

(9) Hitchcock, P. B.; Meidine, M. F.; Nixon, J. F.; Sillet, G. J. D. *J. Chem. Soc., Chem. Commun.* **1990**, 317−319.
(10) Hitchcock, P. B.; Matos, R. M.; Nixon, J. F. *J. Organomet. Chem.* **1993**, *462*, 319−329.
(11) Bartsch, R.; Gelessus, A.; Hitchcock, P. B.; Nixon, J. F. *J. Organomet. Chem.* **1992**, *430*, C10−C14.
(12) Yamazaki, H.; Nishido, T.; Matsumoto, Y.; Sumida, S.; Hagihara, H. *J. Organomet. Chem.* **1966**, *6*, 86−91. Hernandez, E.; Royo, P. *J. Organomet. Chem.* **1985**, *291*, 387−392.
(13) Fischer, E. O.; Jira, R. *Z. Naturforsch.* **1954**, *9b*, 618−619. Feltham, R. D.; Fateley, W. G. *Spectrochim. Acta* **1964**, *20*, 1081.
(14) Bartsch, R.; Hitchcock, P. B.; Madden, T. J.; Meidine, M. F.; Nixon, J. F.; Wang, H. *J. Chem. Soc., Chem. Commun.* **1988**, 1475−1476.
(15) Scheer, M.; Krug, J. *Z. Anorg. Allg. Chem.* **1998**, *624*, 399−405.

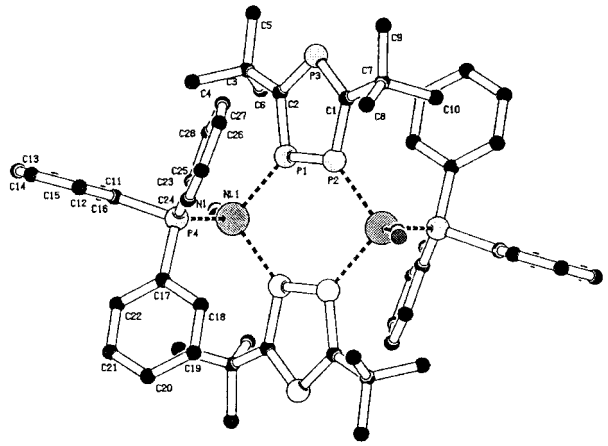

Figure 2. Molecular structure of **6** in the solid state; hydrogen atoms are omitted for clarity.

Scheme 3

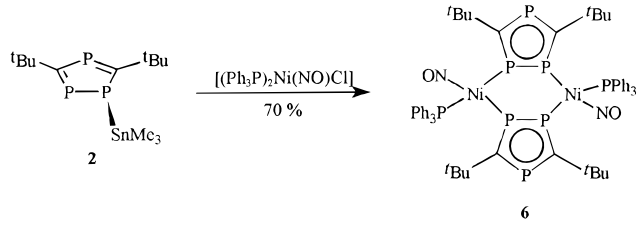

more closely related to the N-heterocyclic Cp analogues pyrazolate or triazolate in this specific example. These ligands prefer σ-coordination.[16] On the other hand, the N-heterocycles are definitely anions if coordinated to transition metals in this manner.[17] If ligand **1** is regarded as an anion in the case of binuclear complex **6**, the NO ligand must be a formal nitrosyl cation. This leads us to view the compound as a classical tetrahedral four-coordinate and diamagnetic 18-VE Ni(0) species.

A temperature-dependent ^{31}P NMR investigation shed more light on the problem of the disagreement between the NMR spectra of solutions of **6** and the structural findings for the solid state. On cooling, the ^{31}P-signals, which are observable at room temperature, remain in the same positions, but decrease in intensity. They are replaced reversibly and quantitatively by a new set of signals, which can be assigned completely to the structure found for **6** in the solid state (Figure 3). Thus, the solid-state dimer **6** is identical with the low-temperature species in solution.

The signals of the ring phosphorus atoms of **6** are clearly separated by 102 ppm, as expected for a σ-bonded ligand **1**,[5] and the ^{31}P signal of PPh_3 is shifted from about -7 ppm to $+36$ ppm, which indicates the complexation to the nickel atoms. At -85 °C more than 90% of the room-temperature species is converted into dimer **6**. As the room-temperature NMR spectra may be

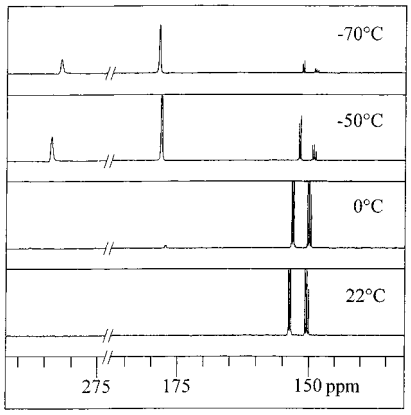

Figure 3. Triphospholyl part of variable-temperature ^{31}P NMR spectra (161.7 MHz) of **6**/**7** in [D_8]toluene.

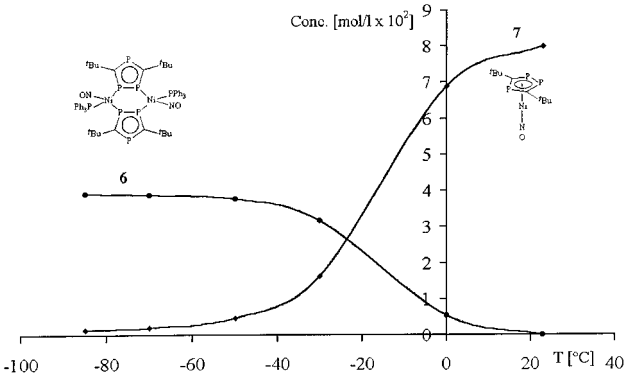

Figure 4. Concentration plot of **6** and **7** as a function of temperature. The data are obtained from the integrated ^{31}P NMR signals. Start concentration 0.04 mol/L **6**.

Scheme 4

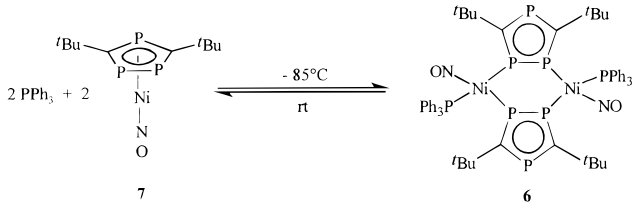

interpreted unambiguously to result from a 1:1 mixture of piano-stool **7** and dissociated PPh_3, the temperature-dependent NMR spectra clearly indicate an equilibrium between **7** and free PPh_3 at the ambient-temperature side, which corresponds to dimer **6** at the low-temperature side (Scheme 4, Figure 4).

Since there is no line broadening observable in the NMR spectra or coalescence between related signals, the speed of the rearrangement reaction is well below the NMR time scale. On the other hand it is rapid enough to reach equilibrium concentrations of the two species within the time requirements for changing the temperature of the NMR sample.

The rearrangement process is assumed to be complex. A minimum of two P−Ni bonds must be cleaved to form a σ-complex monomer out of the dimer. The removal of the PPh_3 ligand may also be correlated to the $\sigma-\pi$-rearrangement of ligand **1** to prevent extremely small electron counts for the reactive intermediates of the process.

Only irreversible $\sigma-\pi$ rearrangements have been reported in the literature for unsaturated P-hetero-

(16) Van Albada, G. A.; De Graaff, R. A. G.; Haasnoot, J. G.; Reedijk, J. *Inorg. Chem.* **1984**, *23*, 1404−1408. Reimann, C. W.; Zocchi, M. *J. Chem. Soc., Chem. Commun.* **1968**, 272. López, G.; Garcia, G.; Sánchez, G.; Garcia, J.; Ruiz, J.; Hermoso, J. A.; Vegas, A.; Martinez-Ripoll, M. *Inorg. Chem.* **1992**, *31*, 1518−1523. Garnowskii, A. D.; Sadimenko, A. P. *Adv. Heterocycl. Chem.* **1999**, *72*, 1−77.

(17) Wilkinson, G.; Gillard, R. D.; McCleverty, J. A. *Comprehensive Coordination Chemistry, The Synthesis, Reactions, Properties and Applications of Coordination Compounds*, Volume 2 Ligands, 1st ed.; Pergamon Press: Oxford, 1987; pp 76−79.

Scheme 5

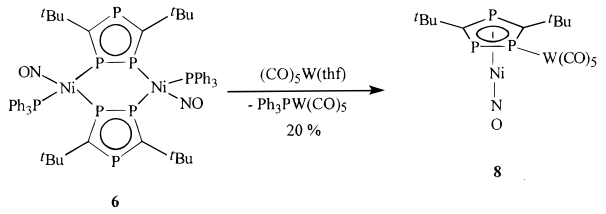

cycles. Phosphabenzene derivatives, for example, may bind metals as η^1- as well as η^6-ligands. The latter coordination mode is the thermodynamically favored one. Nevertheless some σ-complexes are kinetically stabilized and isolable at room temperature. To initiate the $\sigma-\pi$ rearrangement, high temperatures or photochemical conditions are required.[18] There is only one report of a $\sigma-\pi$ rearrangement involving a triphospholyl ligand in the literature. A σ-complex of ligand **1** was observed by ^{31}P NMR to be an unstable intermediate of the formation of $[(\eta^5\text{-}C_5Me_5)(\eta^5\text{-}t\text{-}Bu_2C_2P_3)Ru]$.[19]

While the identity of the dimer **6** is validated by its solid-state structure, the constitution of the monomeric species may be regarded as not fully unambiguous. To prepare pure solutions or crystalline material of **7**, the dissociated PPh_3 was trapped chemically by complexation to a $W(CO)_5$ fragment. Due to the ligand properties of **7**, an excess $(OC)_5W(thf)$ was reacted with the equilibrium mixture of **6**, **7**, and PPh_3. As expected, the reaction results in the formation of monomeric nickel nitrosyl complex **8**, which contains an additional $W(CO)_5$ unit. It is attached to one of the adjacent phosphorus atoms of the triphospholyl ligand (Scheme 5).

The spectroscopic properties of **8** are in agreement with an η^5-coordinated nickel center with an ABC spin system and well-resolved ^{31}P and ^{183}W coupling patterns in ^{31}P NMR. A single-crystal X-ray diffraction study confirmed the molecular structure of $\mu[1{:}1{-}5\text{-}\eta\text{-}t\text{-}Bu_2C_2P_3]$-$\{(CO)_5W\}(NO)Ni\}$, **8** (Figure 5, Table 3).

The Ni−N−O unit is almost linear (175°), and the nitrosyl ligand must be viewed as a three-electron donor. The bond distances are in good agreement with those found for the cyclopentadienyl complex **4**.[20] The structural findings on **8** can be regarded as proof for the proposed structure of **7**. Both are the first one-legged piano-stool complexes of the triphospholyl ligand. As for **5**, the triphospholyl complexes **8** and **7** therefore can be regarded as analogues of their cyclopentadienyl counterparts **3** and **4**.

Conclusions

The ligand 3,5-di(*tert*-butyl)-1,2,4-triphospholyl (**1**) may act as a σ- or π-ligand to nickel atoms, depending on the coligands and thus on the formal oxidation state of the metal and on the temperature. In contrast with a general preference of **1** to act as a π-ligand toward 3d transition metals, the σ-interaction is thermodynamically favored over the η^5-bonding in the case of the nickel nitrosyl complexes. The direct observation of an equilibrium of a reversible $\sigma-\pi$ rearrangement of a P-heterocyclic ligand is as unique as the doubly bridging mode of the heterocyclic ligands within the σ-complex dimer $[\mu,\eta^1{:}\eta^1(t\text{-}Bu_2C_2P_3)(NO)(PPh_3)Ni]_2$ (**6**). **6** is more closely related to bis-pyrazolate or bis-triazolate complexes than to other complexes of unsaturated P-heterocycles or to Cp derivatives. Thus, under the influence of the nitrosyl ligand, the specific interaction between Ni atoms and ligand **1** is fine-tuned in a way that makes a richer chemistry possible than observed for 18-VE CpNi half-sandwich complexes.

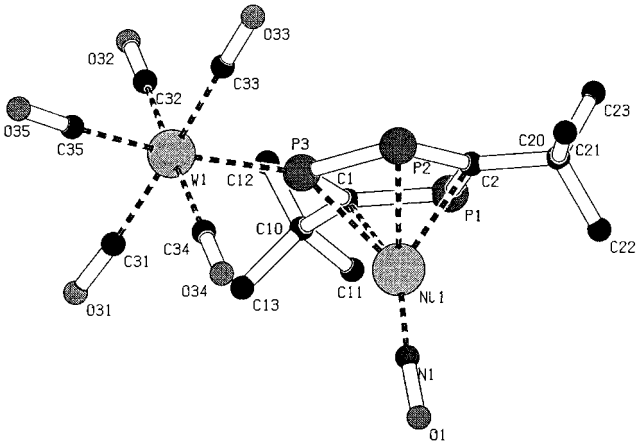

Figure 5. Molecular structure of **8** in the solid state; hydrogen atoms are omitted for clarity.

Experimental Section

General Considerations. All experiments were conducted under nitrogen atmosphere by using standard Schlenk and cannula techniques. Solvents were dried according to described procedures[21] and used freshly distilled from the drying agent. $[(PPh_3)_2NiCl_2]$ was obtained from Fluka Chemie AG; $[(NO)(PPh_3)_2NiCl]$ was prepared according to the literature.[22] 1-Trimethylstannyl-3,5-di(*tert*-butyl)-1,2,4-triphosphole (**2**) was prepared as described previously[7] and distilled in an oil pump vacuum for purification.

$[(\eta^5\text{-}t\text{-}Bu_2C_2P_3)(PPh_3)NiCl]$ (5). A 0.642 g sample of $[(PPh_3)_2NiCl_2]$ (0.981 mmol) is dissolved in 60 mL of dichloromethane. An orange powder starts precipitating after some minutes. A solution of 0.398 g of 1-trimethylstannyl-3,5-di(*tert*-butyl)-1,2,4-triphosphole (**2**) (1.008 mmol) in 40 mL of dichloromethane is added at 0 °C over a period of half an hour. The orange powder redissolves and the color of the solution changes to dark red. The solution is stirred for an additional 10 min, and the volatile parts are removed in a vacuum. The remaining solid is washed repeatedly with *n*-hexane until the solution drains off colorless and dried in vacuo to yield 427 mg (0.727 mmol, 74%) of $[(\eta^5\text{-}t\text{-}Bu_2C_2P_3)(PPh_3)NiCl]$ (**5**).

Spectroscopic Data for 5. ^{1}H NMR (269.7 MHz, $CDCl_3$): δ 1.63 (s, 18H, CH_3), 7.41 (m, 9H, *o*- and *p*-Ph-*H*), 7.78 (m, 6H, *m*-Ph-*H*). $^{31}P\{^1H\}$ NMR (161.7 MHz, CH_2Cl_2, 20.7 °C): δ 219.35 (dt, $^2J(^{31}P,^{31}P) = 30.7$ Hz, $^2J(^{31}P,^{31}P) = 25.9$ Hz, 1P, P_{ring}), 106.87 (d, $^2J(^{31}P,^{31}P) = 25.9$ Hz, 2P, P_{ring}), 26.53 (d, $^2J(^{31}P,^{31}P) = 30.7$ Hz, 1P, PPh_3). $^{13}C\{^1H\}$ NMR (67.83 MHz, $CDCl_3$): δ 35.92 (dpt, $\Sigma\ ^3J(^{31}P,^{13}C) + {}^4J(^{31}P,^{13}C) = 8.0$ Hz, $^3J(^{31}P,^{13}C) = 8.3$ Hz, $C(CH_3)_3$), 40.69 (d, $^2J(^{31}P,^{13}C) = 20.7$ Hz,

(18) Deberitz, J.; Nöth, H. *Chem. Ber.* **1973**, *106*, 2222−2226. Vahrenkamp, H.; Nöth, H. *Chem. Ber.* **1973**, *106*, 2227−2235. Nief, F.; Charrier, C.; Mathey, F.; Simalty, M. *J. Organomet. Chem.* **1980**, *187*, 277−285. Fischer, J.; De Cian, A.; Nief, F. *Acta Crystallogr.* **1981**, *B37*, 1067−1071.

(19) Hitchcock, P. B.; Nixon, J. F.; Matos, R. M. *J. Organomet. Chem.* **1995**, *490*, 155−162.

(20) Ronova, I. A.; Alekseeva, N. V.; Veniaminov, N. N.; Kravers, M. A. *Zh. Strukt. Khim.* **1975**, *16*, 476−478, and literature cited therein.

(21) Perrin, D. D.; Armarego, W. L. F. *Purification of Laboratory Chemicals*, 3rd ed.; Butterworth-Heinemann: Oxford, 1988.

(22) Feltham, R. D. *Inorg. Chem.* **1964**, *3*, 116−119.

Table 1. Selected Bond Length (Å) and Angles (deg) for 5

Ni−Cl	2.2043(5)
Ni−P(4)	2.1779(5)
P(1)−P(2)	2.1839(7)
P(2)−C(1)	1.7429(17)
P(3)−C(1)	1.7584(17)
P(3)−C(2)	1.7672(18)
Ni−P(1)	2.3235(5)
Ni−P(2)	2.3319(5)
Ni−P(3)	2.4032(5)
Ni−C(1)	2.3162(17)
Ni−C(2)	2.2912(17)
P(4)−Ni−Cl	94.056(18)

$C(CH_3)_3$), 128.07 (d, $J(^{31}P,^{13}C) = 10.4$ Hz, *o*- or *m*-Ph-*C*), 130.58 (d, $^4J(^{31}P,^{13}C) = 2.7$ Hz, *p*-Ph-*C*), 132.51 (d, $^1J(^{31}P,^{13}C) = 19.1$ Hz, *i*-Ph-*C*), 134.33 (d, $J(^{31}P,^{13}C) = 9.8$ Hz, *o*- or *m*-Ph-*C*), 188.4 (not res., C_{ring}). MS (FD^+, CH_2Cl_2): *m*/*z* (%) 586 (100) $[M]^+$, 262 (70) $[PPh_3]^+$. Anal. Calcd for ($C_{28}H_{33}ClNiP_4$): C 57.23, H 5.66. Found: C 57.09, H 5.90.

[μ,η^1:η^1(*t*-$Bu_2C_2P_3$)(NO)(PPh_3)Ni]$_2$ (6). A 0.254 g (0.643 mmol) sample of 1-trimethylstannyl-3,5-di(*tert*-butyl)-1,2,4-triphosphole (**2**) in 10 mL of dichloromethane is added at −30 °C to a solution of 0.379 g (0.584 mmol) of [(NO)(PPh_3)$_2$NiCl] in 30 mL of dichloromethane. The color changes from greenish blue to red. After stirring for 30 min at −30 °C and an additional 30 min at room temperature the solvent is removed in vacuo, and the resulting black solid is suspended in cold *n*-hexane, filtered, washed again with cold *n*-hexane until the solution drains off colorless, and dried in vacuo. The solid is dissolved in a minimum amount of a toluene/*n*-hexane mixture, and [μ,η^1:η^1(*t*-$Bu_2C_2P_3$)(NO)(PPh_3)Ni]$_2$ (**6**) precipitates at −18 °C and is separated from the solution, dried, and recrystallized from dichloromethane/*n*-hexane mixtures. Yield of **6**: 0.238 g, 0.204 mmol, 70%.

Spectroscopic Data for 6. $^{31}P\{^1H\}$ NMR (161.7 MHz, [D_8]toluene, −85.2 °C): [AB_2X] spin system, δ 35.9 (s, 1P, *P*Ph_3), 179.1 (s, 2P, P_{ring}), 281.2 (s, 1P, P_{ring}). $^{13}C\{^1H\}$ NMR (100.4 MHz, [D_8]toluene, −84.9 °C): δ 34.70 (s, $C(CH_3)_3$), 40.00 (d, $J(^{31}P,^{13}C) = 22.9$ Hz, $C(CH_3)_3$), 132.5−128 (Ph-*C*, not assigned due to overlapping solvent signals), 202.89 (d, $J(^{31}P,^{13}C) = 65.0$ Hz,C_{ring}). IR (KBr): ν(NO) 1751 cm^{-1}.

Spectroscopic Data for 1:1 Mixtures of 7 and PPh_3. ^1H NMR (399.65 MHz, $CDCl_3$, 23.9 °C): δ 1.65 (s, 18H, CH_3), 7.28−7.35 (m, 15H, C_5H_6). $^{31}P\{^1H\}$ NMR (161.7 MHz, $CDCl_3$, 24.9 °C): [B_2AX] spin system, δ 151.64 (pd, $^2J(^{31}P,^{31}P) = 53.9$ Hz, 2P), 151.0 (pt, $^2J(^{31}P,^{31}P) = 53.9$ Hz, 1P), −5.6 (s, 1P, *P*Ph_3). $^{31}P\{^1H\}$ NMR (161.7 MHz, [D_8]toluene, 22.3 °C): [B_2AX] spin system, δ −5.5 (s, 1P, $P(C_6H_5)_3$), 150.4 (t, $^2J(^{31}P,^{31}P) = 55$ Hz, 1P, P_{ring}), 153.7 (d, $^2J(^{31}P,^{31}P) = 55$ Hz, 2P, P_{ring}). $^{13}C\{^1H\}$ NMR (100.4 MHz, $CDCl_3$, 25.1 °C): δ 36.66 (m, $C(CH_3)_3$), 39.04 (ddd, $^2J(^{31}P,^{13}C) = 16.0$ Hz, $\Sigma\ ^2J(^{31}P,^{13}C) + {}^3J(^{31}P,^{13}C) = 13.6$ Hz, $C(CH_3)_3$), 128.06 (d, $^4J(^{31}P,^{13}C) = 5.7$ Hz, *p*-Ph-*C*), 128.28 (s, *m*-Ph-*C*), 133.32 (d, $^2J(^{31}P,^{13}C) = 19.0$ Hz, *o*-Ph-*C*), 136.78 (d, $^1J(^{31}P,^{13}C) = 10.7$ Hz, *i*-Ph-*C*), 179.35 (ddd, $^1J(^{31}P,^{13}C) = 77.2$ Hz, $\Sigma\ ^1J(^{31}P,^{13}C) + {}^2J(^{31}P,^{13}C) = 109.8$ Hz, C_{ring}). IR (*n*-hexane): ν(NO) 1824 cm^{-1}. MS (FD^+, CH_2Cl_2): *m*/*z* (%) 262 (100) $[PPh_3]^+$, 319 (40) $[(t\text{-}Bu_2C_2P_3)Ni(NO)]^+$.

μ[1:1−5-η-*t*-$Bu_2C_2P_3$]{$(CO)_5W$}(NO)Ni} (8). A 172 mg (0.148 mmol) sample of {μ[1:2-η-t-$Bu_2C_2P_3$](NO)(PPh_3)Ni}$_2$ (**30**) is reacted at −40 °C with 0.86 mmol of freshly prepared $(CO)_5$(thf)W in 250 mL of THF. The black-green suspension is allowed to reach room temperature, and a clear red solution forms. After ca. 4 h the reaction is completed (checked by IR monitoring). The solvent is removed in vacuo, the residue is dissolved in *n*-hexane and filtered, and the solution is concentrated to 30 mL and stored overnight at −18 °C. Clear crystals form. The brownish-red solution is separated via syringe and the crystals are washed twice with 5 mL of −30 °C *n*-hexane. The combined solutions are reduced in vacuo and column chromatographed on SiO_2/5% H_2O. With *n*-hexane as eluent 38 mg (0.059 mmol, 20.0%) of μ[1:1−5-η-*t*-$Bu_2C_2P_3$]{$(CO)_5W$}(NO)Ni} (**8**) is obtained as a red oil.

Table 2. Selected Bond Length (Å) and Angles (deg)[a] for 6

Ni(1)−Ni(1#)	4.745(1)
Ni(1)−N(1)	1.662(3)
Ni(1)−P(1)	2.2626(11)
Ni(1)−P(2#)	2.2874(11)
Ni(1)−P(4)	2.3304(11)
P(1)−P(2)	2.0823(14)
P(1)−C(2)	1.746(4)
P(2)−C(1)	1.741(4)
P(3)−C(1)	1.744(4)
P(3)−C(2)	1.744(4)
N(1)−O(1)	1.169(5)
N(1)−Ni(1)−P(1)	107.44(12)
N(1)−Ni(1)−P(2#)	111.67(12)
P(1)−Ni(1)−P(2#)	101.74(4)
N(1)−Ni(1)−P(4)	124.56(12)
P(1)−Ni(1)−P(4)	105.50(4)
P(2#)1−Ni(1)−P(4)	103.54(4)
Ni(1)−P(1)−P(2)	119.92(6)
Ni(1)−N(1)−O(1)	166.4(3)
P(1)−P(2)−C(1)	100.71(14)
P(2)−P(1)−C(2)	100.98(14)
P(1)−C(2)−P(3)	117.1(2)
P(2)−C(1)−P(3)	117.5(2)
C(2)−P(3)−C(1)	103.57(18)

[a] # indicates symmetry equivalent atoms, symmetry transformations used to generate equivalent atoms: $-x+1,-y+1,-z+1$.

Table 3. Selected Bond Length (Å) and Angles (deg) for 8

Ni−N	1.613 (17)
N−O(1)	1.14 (2)
P(2)−P(3)	2.119 (6)
P(2)−C(2)	1.754 (18)
P(3)−C(1)	1.776 (17)
P(1)−C(1)	1.763 (17)
P(1)−C(2)	1.772 (18)
Ni−P(1)	2.341 (5)
Ni−P(2)	2.396 (5)
Ni−P(3)	2.371 (5)
Ni−C(1)	2.222 (16)
Ni−C(2)	2.194 (17)
P(3)−W	2.495 (4)
C−O (mean)	1.15 (2)
Ni−N−O(1)	175.2 (18)

Spectroscopic Data for 8. ^1H NMR (269.72 MHz, C_6D_6): δ 1.521 (s, 9H, CH_3), 1.316 (s, 9H, CH_3). $^{31}P\{^1H\}$ NMR (161.7 MHz, C_6D_6, 22.5 °C): [ABC] spin system, δ 140.6 (dd, $^2J(^{31}P,^{31}P) = 46.9$ Hz, $^2J(^{31}P,^{31}P) = 55.8$ Hz, 1P), 126.56 (dd, $^1J(^{31}P,^{31}P) = 422.0$ Hz, $^2J(^{31}P,^{31}P) = 46.9$ Hz, 1P), 116.86 (d, $^1J(^{183}W,^{31}P) = 224.0$ Hz, dd, $^1J(^{31}P,^{31}P) = 422.0$ Hz, $^2J(^{31}P,^{31}P) = 55.8$ Hz, 1P). $^{13}C\{^1H\}$ NMR (100.40 MHz, C_6D_6, 21.7 °C): δ 198.66 (d, $^1J(^{183}W,^{13}C) = 151.9$ Hz, d, $^2J(^{31}P,^{13}C) = 32.0$ Hz, *C*O), 196.35 (d, $^1J(^{183}W,^{13}C) = 126.3$ Hz, d, $^2J(^{31}P,^{13}C) = 2.7$ Hz, *C*O), 175.17 (dd, $^1J(^{13}C,^{31}P) = 83.7$ Hz, $^1J(^{13}C,^{31}P) = 92.2$ Hz, $^2J(^{13}C,^{31}P) = 6$ Hz, C_{ring}), 166.81 (dd, $^1J(^{13}C,^{31}P) = 67.7$ Hz, $^1J(^{13}C,^{31}P) = 86.0$ Hz, $^2J(^{13}C,^{31}P) = 11.6$ Hz, C_{ring}), 39.2 (m, $C(CH_3)_3$), 36.2 (m, $C(CH_3)_3$). IR (*n*-hexane): ν(CO) 2076 (m), 1955 (s), ν(NO) 1832 (s) cm^{-1}. MS (FD^+, *n*-hexane): *m*/*z* (%) 644 (100) $[M]^+$.

Crystal Structure Determination of 5 and 6. Crystal data were collected on a Bruker AXS SMART 1000 diffractometer with CCD area detector (Mo Kα radiation, graphite monochromator, $\lambda = 0.71073$ Å) at −100 °C using SMART software.[23] The reflection intensities were integrated using

(23) *SMART* and *SAINT, NT V5.0*, Area detector control and integration software; Bruker AXS: Madison, WI, 1999.

Table 4. Crystal Data and Structure Refinement of 5, 6, and 8

	5	6	8
empirical formula	$C_{28}H_{33}ClNiP_4$	$C_{56}H_{66}N_2Ni_2O_2P_8$	$C_{15}H_{18}NNiO_6P_3W$
fw	587.58	1164.29	643.77
solvent	*n*-hexane/CH_2Cl_2	*n*-hexane/CH_2Cl_2	*n*-hexane
cryst habit	black fragment	black fragment	red plate
temperature	173(2) K	173(2) K	220(2) K
cryst syst	monoclinic	triclinic	monoclinic
space group	$P2_1/n$	$P\bar{1}$	$C2/c$
unit cell dimens	$a = 15.9255(7)$ Å	$a = 10.7894(2)$ Å	$a = 15.628(6)$ Å
	$b = 10.7772(5)$ Å	$b = 11.1402(2)$ Å	$b = 10.000(3)$ Å
	$c = 16.9237(8)$ Å	$c = 12.4640(3)$ Å	$c = 29.138(10)$ Å
	$\alpha = 90°$	$\alpha = 102.940(1)°$	$\alpha = 90°$
	$\beta = 97.531(1)°$	$\beta = 101.216(1)°$	$\beta = 90.43(3)°$
	$\gamma = 90°$	$\gamma = 101.606(1)°$	$\gamma = 90°$
volume	2879.6(2) Å^3	1384.47(5) Å^3	4554(3) Å^3
Z	4	1	8
density (calcd)	1.355 g/cm^3	1.396 g/cm^3	1.878 g/cm^3
abs coeff	1.004 mm^{-1}	0.954 mm^{-1}	6.114 mm^{-1}
$F(000)$	1224	608	2480
cryst size	0.44 × 0.25 × 0.16 mm	0.43 × 0.11 × 0.04 mm	0.50 × 0.24 × 0.04 mm
θ range for data collection	1.65−28.29°	1.73−28.31°	2.42−26.02°
index ranges	$-21 \le h \le 20$,	$-14 \le h \le 13$,	$-19 \le h \le 1$,
	$0 \le k \le 14$,	$-14 \le k \le 14$,	$-12 \le k \le 1$,
	$0 \le l \le 21$	$0 \le l \le 16$	$-35 \le l \le 35$
no. of reflns collected	16 925	18 698	5279
no. of ind reflns	6850 [R(int) = 0.028]	6765 [R(int) = 0.049]	4278 [R(int) = 0.088]
no. of reflns with $I > 2\sigma(I)$	5456	5118	2552
completeness to $\theta = 28.3°$	95.6%	98.0%	94.9%
abs corr	semiempirical from equivalents		semiempirical from ψ-scans
max. and min. transmn	0.894 and 0.689	0.928 and 0.744	0.399 and 0.937
refinement method	full-matrix least-squares on F^2		
no. of data/restraints/params	6850/0/439	6765/0/324	4278/0/250
goodness-of-fit on F^2	0.975	1.081	1.049
final R indices [$I > 2\sigma(I)$]	R1 = 0.029, wR2 = 0.071	R1 = 0.051, wR2 = 0.136	R1 = 0.072, wR2 = 0.162
R indices (all data)	R1 = 0.042, wR2 = 0.075	R1 = 0.070, wR2 = 0.141	R1 = 0.136, wR2 = 0.196
largest diff peak and hole	0.54 and −0.23 e Å^{-3}	0.98 and −0.38 e Å^{-3}	1.76 and −1.68 e Å^{-3}

SAINT [23] and corrected for absorption using SADABS.[24] The structures were solved by direct methods and refined by full-matrix least-squares against F^2 with all reflections using SHELXTL-programs.[25] All non-hydrogen atoms were refined anisotropically. All hydrogen atoms were located in difference Fourier maps and refined isotropically. Crystal data and experimental details are listed in Table 4.

Crystal Structure Determination of 8. Intensity data were collected on a Siemens P4 diffractometer (ω scan technique, 6.0°/min, Mo Kα radiation, graphite monochromator, λ = 0.71073 Å) at 220 K using the XSCAnS 2.20[26] software. The structure was solved by direct methods and refined by full-matrix least-squares against F^2 with all reflections using SHELXTL-programs.[25] All non-hydrogen atoms were refined anisotropically. All hydrogen atoms are geometrically positioned. Crystal data and experimental details are listed in Table 4.

All peaks of significant residual electron density are to be found close to the W atom.

Acknowledgment. This work was supported by the Deutsche Forschungsgemeinschaft and the Fonds der Chemischen Industrie. M.Z. is grateful for a scholarship by the DFG-Graduiertenkolleg Phosphorchemie als Bindeglied verschiedener chemischer Disziplinen, at the University of Kaiserslautern, Germany. We also thank Dr. M. Moll for the measurement of variable-temperature NMR spectra.

Supporting Information Available: Further details of the structure determination including tables of atomic coordinates, bond distances and angles, and thermal parameters. This material is available free of charge via the Internet at http://pubs.acs.org.

OM000326G

(24) Sheldrick, G. M. *SADABS, Program for scaling and correction of area detector data*; Göttingen, 1996.

(25) Sheldrick, G. M. *SHELXTL NT V5.1*; Bruker AXS: Madison, WI, 1999.

(26) *XSCANS 2.20*; Siemens Analytical X-ray Instruments: Madison, WI, 1996.